Coherence in neutrino oscillations

Joonas Ilmavirta

Kandidaatin tutkielma
Jyväskylän yliopisto, Fysiikan laitos
4.2.2011
Ohjaaja: Jukka Maalampi

Abstract

The theory of neutrino oscillations has turned out to be the most reasonable explanation to the observed violations in lepton number conservation of solar and atmospheric neutrino fluxes. A derivation of the most important results of this theory is first given using a plane wave treatment and subsequently using a three-dimensional shape-independent wave packet approach. Both methods give the same oscillation patterns, but only the latter one serves as a decent starting point for analyzing coherence in neutrino oscillations.

A numerical analysis of the oscillation patterns on various distance scales is also given to graphically illustrate the phenomenon of neutrino oscillation and loss of coherence in it.

Several coherence conditions related to wave packet separation and the uncertainties of energy and momentum in the mass states produced in a weak charged current reaction are derived. In addition, a new limit is obtained for neutrino flux, beyond which the oscillation pattern may be washed out due to the overlap of the wave packets describing neutrinos originating from different reactions. Whether or not any phenomena will take place in the case of very high flux remains uncertain, because the flux limit is beyond the scope of any modern neutrino experiment.

Tiivistelmä

Neutriino-oskillaatiot tarjoavat luontevimman selityksen havaituille leptonilukujen säilymislain rikkoutumiselle, joka on havaittu auringosta ja ilmakehästä tulevissa neutriinoissa. Neutriino-oskillaatioiden teorian tärkeimmät tulokset johdetaan ensin tasoaaltoapproksimaatiossa ja sen jälkeen käyttäen kolmiulotteisia mielivaltaisen muotoisia aaltopaketteja. Oskillaatiota ja siihen liittyvää koherenssin häviämistä havainnollistetaan numeerisilla laskuilla tuotetuin kuvaajin.

Oskillaatioille johdetaan erilaisia koherenssiehtoja liittyen aaltopakettien erkanemiseen sekä energian ja liikemäärän epätarkkuuteen. Lisäksi löydetään uusi raja neutriinovuolle, jonka yläpuolella oskillaatiot saattavat kadota. Se, tapahtuuko näin suurilla voilla kiinnostavia ilmiöitä, jää epävarmaksi, sillä nykyisillä koejärjestelyillä asiaa ei ole mahdollista tutkia.

Summarium

Violatio observata conservationis numerorum leptorum in neutrinis de Sole et atmosphaera devolantibus simplicissime explicari potest oscillatione neutrinorum. Eventus principales theoriae oscillationum neutrinorum deducuntur primum undulis planis, deinde fascibus undulatoriis tridimensionalibus cuiuslibet formae. Oscillatio amissioque cohaerentiae in ea graphice illustrantur.

Variae necessitates cohaerentiae ad dissociationem fascium undulatoriorum et incertitatem energiae et motus pertinentes deducuntur, necnon novus finis flumini neutrinonum, super quem oscillationes abolescere possunt. An vero abolescant necne, incertum relinquitur, quia tale flumen longe extra facultates hodiernas mensurandi manet.

Contents

1 Introduction

Despite the great success of the Standard Model (SM), not all of its predictions are in accordance with phenomena observed in Nature. It has turned, contrary to the predictions of SM, out that neutrinos do have mass and that none of the three lepton numbers is conserved — in the case of sterile neutrinos even the sum of these three lepton numbers is not conserved. Indeed, neutrino oscillations were the first evidence that something must be lacking from the SM [1]. New theoretical ideas are needed to explain these phenomena.

Observations of atmospheric and solar neutrinos indicate violations in lepton number conservation. In the former case, the observed flux of muon neutrinos ν_μ on the ground is substantially smaller than what is estimated to be produced in interactions of cosmic rays in the atmosphere. In the latter case a fraction of the electron neutrinos created in the Sun seems to disappear on its way to Earth (for experimental results, see eg. [2]), which was known as the solar neutrino problem (for a more thorough discussion of neutrino astronomy, see [3]). In both phenomena some of the produced neutrinos transform into neutrinos of other flavors as they propagate through space, and they are thus merely two incarnations of the same phenomenon, neutrino oscillation.

The most natural explanation to this and other observed phenomena unpredicted by the sole SM arises from the concept of mixed and massive neutrinos [4]. According to this explanation, the weak interaction eigenstates $|\nu_e\rangle$, $|\nu_\mu\rangle$, and $|\nu_\tau\rangle$ (i.e. the flavor states) have no well-defined mass, but their superpositions do. The flavor states $|\nu_\alpha\rangle$ ($\alpha = e, \mu, \tau$) are expressed in terms of the mass states $|\nu_i\rangle$ as [5]

$$|\nu_\alpha\rangle = \sum_{i=1}^{N} U^*_{\alpha i} \, |\nu_i\rangle \, , \tag{1}$$

where U is the neutrino mixing matrix or the Pontecorvo–Maki–Nakagawa–Sakata matrix [6]. The matrix U is unitary and can be chosen real and orthogonal if there is no CP-violation in neutrino mixing [7, 8]. For definiteness, the mixing matrix U is taken to be a unitary but not necessarily real 3×3-matrix. Both the flavor and mass neutrino states are orthonormal, $\langle \nu_\alpha | \nu_\beta \rangle = \delta_{\alpha\beta}$ and $\langle \nu_i | \nu_j \rangle = \delta_{ij}$.

A flavor antineutrino state $|\bar{\nu}_l\rangle$ can be expressed in terms of antineutrino mass states as [9]

$$|\bar{\nu}_\alpha\rangle = \sum_{i=1}^{N} U_{\alpha i} \, |\bar{\nu}_i\rangle \, , \tag{2}$$

where the only change to Eq. (1) is the absence complex conjugation in the mixing matrix elements. If the mixing matrix is taken to be real, the mixing

schemes for neutrinos and antineutrinos are exactly the same. The time evolution of an antiparticle state is similar to that of a particle state[1], so the oscillation pattern will be the same. Therefore only neutrinos will be considered in the following.

An analogue of neutrino mixing is found in classical mechanics: the mass states can be identified with normal coordinates in a system of coupled oscillators, whereas flavor states describe individual oscillators. The obtained oscillation phenomenon bears a striking resemblance to that of neutrino oscillations, although quantum mechanics or quantum field theory is needed to describe neutrinos. A nice discussion of classical coupled oscillators is given in [10].

The flavor space — which is the state space in the crudest approximation — is usually taken to be three-dimensional. If $N > 3$, there are sterile neutrinos, "flavors" that do not enter the SM electroweak interaction Lagrangian and therefore do not interact [6]. On the basis of experimental data it is not yet possible to conclude whether sterile neutrinos exist or not [11].

The origin and exact values of the neutrino masses is a vast area of theoretical [12] and experimental [11] research, which will not be dwelled into in any more detail than required for the other considerations.

It is not even known whether neutrinos are Dirac or Majorana particles. In the latter case neutrinos are their own antiparticles and in the former case not [12]. Other standard model fermions are known to be Dirac particles, but it is believed that neutrinos make an exception.

2 Plane wave approximation

2.1 The standard formula for neutrino oscillations

The simplest insight to neutrino oscillations is provided by the study of the time evolution of flavor plane waves. In fact, even the formalism of plane waves simplifies to a three-state system of the flavor neutrinos, and the spatial dependence of the phenomenon is later introduced by an *ad hoc* procedure.

As the flavor neutrino states have no well-defined mass, they have no well-defined energy and therefore their time dependence is more complex than that of a simple phase factor. The mass states do, however, have the most simple time evolution.

Consider a neutrino state $|\nu(t)\rangle$ and assume that it is created at $t = 0$ as a pure flavor state of flavor α, i.e. $|\nu(0)\rangle = |\nu_\alpha\rangle$. As stated in Eq. (1), this

[1] For a particle state $|\phi(t)\rangle = e^{-iEt}\,|\phi\rangle$ and for an antiparticle $|\phi(t)\rangle = e^{+iEt}\,|\phi\rangle$. Complex conjugating all phases in the calculations will lead to the same absolute values of inner products.

state is the superposition of massive neutrinos,

$$|\nu(0)\rangle = \sum_{i=1}^{3} U^*_{\alpha i} |\nu_i\rangle \,. \tag{3}$$

Given that the mass state $|\,\nu_i\rangle$ has the energy E_i, the time evolution of the state is simply given by

$$|\nu(t)\rangle = \sum_{i} U^*_{\alpha i} e^{-iE_i t} |\nu_i\rangle \,. \tag{4}$$

The bra vector corresponding to the neutrino of flavor β is found by conjugating (1):

$$\langle\nu_\beta| = \sum_{j} U_{\beta j} \langle\nu_j| \,. \tag{5}$$

Thus the probability of finding a neutrino in the flavor β at a time t is given by

$$P(\nu_\alpha \to \nu_\beta; t) = |\langle\nu_\beta|\nu(t)\rangle|^2 = \sum_{i,j} U^*_{\alpha i} U_{\beta j} U_{\alpha j} U^*_{\beta j} e^{-i(E_i t - E_j t)}. \tag{6}$$

2.2 Massive neutrinos of equal energy

A crucial but dubious step in the calculation of the probability is to introduce relations between the properties of different neutrinos mass states and between time and space. This transforms the flavor detection probability function in Eq. (6) into a function of distance and a kinematical variable describing the produced neutrino.

A common way to do this is to assume that all the neutrino mass states have the same energy. Arguments supporting this idea are presented, for example, in [13, 14, 15], although some consider it unphysical [5]. These arguments will be discussed more thoroughly in section 2.4.

Elementary relativistic kinematics shows that a particle of mass m and energy E travels at the speed

$$v = \sqrt{1 - \frac{m^2}{E^2}}. \tag{7}$$

If L is the distance traveled by the neutrino between production and detection points and every massive neutrino has the energy E, then

$$\begin{aligned} Et_i - Et_j &= EL\left(1 - \frac{m_i^2}{E^2}\right)^{-1/2} - EL\left(1 - \frac{m_j^2}{E^2}\right)^{-1/2} \\ &\approx EL\left(1 + \frac{m_i^2}{2E^2}\right) - EL\left(1 + \frac{m_j^2}{2E^2}\right) \\ &= \frac{L(m_i^2 - m_j^2)}{2E}, \end{aligned} \tag{8}$$

which is accurate to the first order in squared neutrino masses. Denoting $\Delta m^2_{ij} = m^2_i - m^2_j$, Eq. (6) leads to the standard formula for neutrino oscillations:

$$P(\nu_\alpha \to \nu_\beta; L) = \sum_{i,j} U^*_{\alpha i} U_{\beta i} U_{\alpha j} U^*_{\beta j} e^{-i\frac{L\Delta m^2_{ij}}{2E}}. \tag{9}$$

2.3 Massive neutrinos of equal momentum

Some authors consider the equal energy assumption unphysical [5] and instead assume that the different mass states have the same momentum instead. Some [7] use the assumption for other than physical reasons such as simplicity. These different assumptions of equal energy or momentum have little or no difference in either the difficulty of the calculations or the result.

Let every mass state $|\nu_i\rangle$ in Eq. (4) have the same momentum p. The energies of the states are then

$$E_i = \sqrt{p^2 + m^2_i} \approx p + \frac{m^2_i}{2p} \tag{10}$$

and so

$$E_i t - E_j t \approx \frac{t\Delta m^2_{ij}}{2p}. \tag{11}$$

If one further assumes that $L \approx t$, i.e. $v \approx 1$, one arrives to the formula

$$P(\nu_\alpha \to \nu_\beta; L) = \sum_{i,j} U^*_{\alpha i} U_{\beta i} U_{\alpha j} U^*_{\beta j} e^{-i\frac{L\Delta m^2_{ij}}{2p}}, \tag{12}$$

which only differs from Eq. (9) in that E has been replaced by p. Bearing in mind that $E \approx p$ for ultrarelativistic neutrinos, these two results are the same in the approximation used. Since $L\Delta m^2_{ij}/2p$ is already first order in squared neutrino masses, the corrections from changing p to E are negligible.

Some authors think that these two approaches give exactly the same result and represent essentially the same physics, although it may be better to distinguish these two approaches [16]. This comparison is, however, beyond the scope of the present analysis.

2.4 An overview to the physics behind the assumptions

Plane waves are not localized, and in fact even non-propagating [17], but one does wish to calculate distance-dependent probabilities in order to be able to make predictions for neutrino oscillation experiments.

In the above derivation of the oscillation probability formula it was necessary to assume that the mass states have either equal energy or equal momentum. It sounds plausible that they are both *almost* equal. As the

wave packet treatment will show, this is sufficient to obtain the standard formula of Eq. (9).

Even if massive neutrinos have equal energy or equal momentum in some frame of reference, they will not in general do so after a Lorentz boost [9]. Therefore assumptions of equal momentum or equal energy are valid only in the framework of a specific frame. Defining such a frame is a dubious *ad hoc* procedure. In the wave packet treatment no such assumption is needed to arrive at the probability formula (9). In a generic case of three flavor neutrinos there will be no frame where the massive neutrinos have equal energy [17]. Frame independence allows for much more flexibility in applying the theory to any practical situation.

Coherence can only be given a rigorous treatment using wave packets, and this will be done in section 4. A simplified coherence condition will be derived in terms of the plane wave approximation, but such a model cannot properly describe the coherence of massive neutrinos at a given time and point.

A general assumption made in most neutrino oscillation investigations is that neutrinos are ultrarelativistic. Not all neutrinos need be, but since only neutrinos of about 100 keV or more energy can be observed [5] and neutrino masses are at most around 2 eV [11], this approximation is very good for all observable neutrinos of the stardard type.

3 Wave packets

3.1 The need for the wave packet treatment

As discussed in Section 2.4, the plane wave approximation requires numerous physically questionable assumptions. Usually neutrinos have neither equal energy nor equal momentum [9], and with wave packets no such assumption is needed. Also, no trajectory condition such as $L \approx t$ needs to be imposed by hand, because such a trajectory equation can be *derived* from the time evolution of the wave packets.

There are two highly unphysical consequences of approximating neutrinos by plane waves. First, in this approach the neutrino has a well-defined momentum and thus completely loses its locality. Second, the source of a plane wave has to vibrate in the same manner for in infinite period of time [18]. It is easy to understand that the production process of a neutrino is spatially localized and spans only over a finite period of time.

3.2 Wave packet spreading

Wave packet spreading can be analyzed [16] by considering a wave function in the momentum representation having a Gaussian wave packet form

$$f(p) = \frac{1}{\sqrt{\sqrt{\pi}\sigma_p}} \exp\left(\frac{(p-p_0)^2}{2\sigma_p^2}\right), \tag{13}$$

where p_0 is the mean momentum and σ_p is the momentum uncertainty. From this the corresponding wave function in coordinate representation is obtained by Fourier transform:

$$\psi(x,t) = \frac{1}{\sqrt{2\pi}} \int \mathrm{d}p f(p) e^{i(px-Et)}. \tag{14}$$

Assuming that the particle in question has a mass m, the energy of the particle is $E = E(p) = \sqrt{p^2+m^2}$. Denoting $E_0 = E(p_0)$, this expression is expanded around the peak of $f(p)$ as

$$E(p) \approx E_0 + \left.\frac{\mathrm{d}E}{\mathrm{d}p}\right|_{p=p_0} (p-p_0) + \left.\frac{\mathrm{d}^2E}{\mathrm{d}p^2}\right|_{p=p_0} \frac{(p-p_0)^2}{2}. \tag{15}$$

Expanding only to the first order gives wave packets of constant shape, while the second order term allows one to analyze the spreading [16]. Carrying out the differentiations and introducing $v = p_0/E_0$ (the group velocity of the particle as discussed in Section 3.3.1), the energy becomes

$$E(p) \approx E_0 + v(p-p_0) + \frac{1-v^2}{E_0}\frac{(p-p_0)^2}{2}. \tag{16}$$

Collecting Eqs. (13), (14), and (16) and carrying out the integration yields

$$\begin{aligned}\psi(x,t) \approx{}& \frac{1}{\sqrt[4]{\pi}} \sqrt{\frac{p_0\sigma_p}{p_0 + i\sigma_p^2 tv(1-v^2)}} \\ &\times \exp\left(\frac{\frac{2ip_0t}{v} + \sigma_p^2t^2(3v^2-2) - (2ip_0 + 2\sigma_p^2tv^3)x + \sigma_p^2x^2}{2p_0^{-1}(p_0 + i\sigma^2tv(1-v^2))}\right).\end{aligned} \tag{17}$$

The squared modulus of the wave function $\psi(x,t)$ gives the transition probability density ρ,

$$\begin{aligned}\rho(x,t) ={}& \frac{1}{\sqrt{\pi}} \frac{p_0\sigma_p}{\sqrt{p_0^2 + \sigma_p^4t^2v^2(1-v^2)^2}} \\ &\times \exp\left(-\frac{(x-tv)^2}{\sigma_p^{-2}(1 + \sigma_p^4t^2v^2\,(1-v^2)^2\,/p_0^2)}\right).\end{aligned} \tag{18}$$

This implies that the length of the wave packet σ_x behaves as

$$\sigma_x(t) = \sigma_{x0}\sqrt{1 + \frac{\sigma_p^4 t^2 v^2 \left(1 - v^2\right)^2}{p_0^2}}. \tag{19}$$

The application of this result to neutrino oscillations will be discussed in Section 4.5.

3.3 Neutrino oscillations in wave packet treatment[2]

3.3.1 Produced and detected states

Neutrino oscillations are now considered in wave packet formalism as opposed to the plane waves used in Section 2. As in the plane wave approach, a flavor neutrino state of flavor α is created at the origin of a frame of reference when $t = 0$. The corresponding state is decomposed to massive neutrino states, which are described by wave packets $\psi_i^S(\vec{x}, t)$ (superscript S refers to the source):

$$|\nu(\vec{x}, t)\rangle = \sum_i U_{\alpha i}^* \psi_i^S(\vec{x}, t) \, |\nu_i\rangle \,, \tag{20}$$

where the wave packets are described by momentum distribution functions $f_i^S(\vec{p})$ as

$$\psi_i^S(\vec{x}, t) = \int \frac{\mathrm{d}^3\vec{p}}{(2\pi)^{3/2}} f_i^S(\vec{p} - \vec{p}_i^S) e^{i(\vec{p}\cdot\vec{x} - E_i(p)t)}, \tag{21}$$

where $\vec{p}_i^S$ is the mean momentum and $E_i(p) = \sqrt{p^2 + m_i^2}$.

In the above the function $f_i^S(\vec{p})$ is strongly peaked at the origin; taking $f_i^S(\vec{p}) = \delta^{(3)}(\vec{p})$ would lead to plane waves with definite momenta. It is also assumed that the peak of $f_i^S(\vec{p} - \vec{p}_i^S)$ is not near the origin, that is $\sigma_{p_i}^S \ll p_i^S$. This can be justified by the ultrarelativistic nature of detectable neutrinos.

Since the above integral is assumed to be strongly suppressed outside $\vec{p} \approx \vec{p}_i^S$, one may expand the energy as

$$E_i(p) = E_i(p_i^S) + \left.\frac{\partial E_i(p)}{\partial \vec{p}}\right|_{\vec{p}_i^S} \cdot (\vec{p} - \vec{p}_i^S). \tag{22}$$

Differentiating $E_i(p)$ gives

$$\left.\frac{\partial E_i(p)}{\partial \vec{p}}\right|_{\vec{p}_i^S} = \frac{\vec{p}_i^S}{E_i(p_i^S)}. \tag{23}$$

This derivative is the group velocity $\vec{v}_{gi}$ of the wave packet.

[2] This discussion mostly follows that of [17].

Working to the first order squared neutrino masses, one may write $\vec{p}\cdot\vec{x} - E_i(p)t = \vec{p}_i^S\cdot\vec{x} + (\vec{p}-\vec{p}_i^S)\cdot\vec{x} - (E_i(p_i^S) + \vec{v}_{gi}\cdot(\vec{p}-\vec{p}_i^S))t$, and thus the wave packet (21) can be rewritten as

$$\psi_i^S(\vec{x},t) = e^{i(\vec{p}_i^S\cdot\vec{x} - E_i(p_i^S))} g_i^S(\vec{x}-\vec{v}_{gi}t), \tag{24}$$

where

$$g_i^S(\vec{x}) = \int \frac{\mathrm{d}^3\vec{p}}{(2\pi)^{3/2}} f_i^S(\vec{p}) e^{i\vec{p}\cdot\vec{x}}. \tag{25}$$

In this approximation the shape of the wave packet is preserved [17]. This is evident from the fact that the shape factor of the wave packet depends on time and place only through the combination $\vec{x}-\vec{v}_{gi}t$ — this form also explains why $\vec{v}_{gi}$ is the group velocity.

A detecting particle is placed at $\vec{x}=\vec{L}$. In most cases of interest, the detected neutrino state $|\nu_\beta\rangle$ is essentially time-independent [17]. Thus, we have in analogue to to the state $|\nu(\vec{x},t)\rangle$ discussed above (D refers to the detecting particle),

$$\left|\nu_\beta(\vec{x}-\vec{L})\right\rangle = \sum_i U_{\beta i}^* \psi_i^D(\vec{x}-\vec{L})\,|\nu_i\rangle \tag{26}$$

$$\psi_i^D(\vec{x}-\vec{L}) = \int \frac{\mathrm{d}^3\vec{p}}{(2\pi)^{3/2}} f_i^D(\vec{p}-\vec{p}_i^D) e^{i\vec{p}\cdot(\vec{x}-\vec{L})}. \tag{27}$$

It is assumed that the momentum distribution functions f_i^D are strongly peaked around the origin. As above, the wave packet can be approximated as

$$\psi_i^D(\vec{x}-\vec{L}) = e^{i\vec{p}_i^D\cdot(\vec{x}-\vec{L})} g_i^D(\vec{x}-\vec{L}), \tag{28}$$

where

$$g_i^D(\vec{x}) = \int \frac{\mathrm{d}^3\vec{p}}{(2\pi)^{3/2}} f_i^D(\vec{p}) e^{i\vec{p}\cdot\vec{x}}. \tag{29}$$

3.3.2 From transition amplitude to probability

By projecting the produced, time-evolved neutrino state (20) to the detected state (26), one arrives at the transition amplitude

$$\mathcal{A}_{\alpha\to\beta}(\vec{L},t) = \int \mathrm{d}^3\vec{x} \left\langle \nu_\beta(\vec{x}-\vec{L})\right| \left|\nu(\vec{x},t)\right\rangle. \tag{30}$$

In order to evaluate this amplitude, one has to evaluate integrals of the form

$$\int \mathrm{d}^3\vec{x}\,\psi_i^{D*}(\vec{x}-\vec{L})\psi_i^S(\vec{x},t). \tag{31}$$

Using the expressions (24) and (28) and noting that

$$(\vec{p}_i^S\cdot\vec{x} - E_i(p_i^S)t) - \vec{p}_i^D\cdot(\vec{x}-\vec{L}) = \vec{p}_i^S\cdot\vec{L} - E_i(p_i^S)t + (\vec{p}_i^S-\vec{p}_i^D)\cdot(\vec{x}-\vec{L}), \tag{32}$$

one may write

$$\psi_i^{D*}(\vec{x}-\vec{L})\psi_i^S(\vec{x},t) = g_i^{D*}(\vec{x}-\vec{L})g_i^S(\vec{x}-\vec{v}_{gi}t)e^{i(\vec{p}_i^S\cdot\vec{L}-E_i(p_i^S)t)}e^{i(\vec{p}_i^S-\vec{p}_i^D)\cdot(\vec{x}-\vec{L})}. \tag{33}$$

The orthogonality of massive neutrino states gives then for the transition amplitude $\mathcal{A}_{\alpha\to\beta}$ the form

$$\mathcal{A}_{\alpha\to\beta}(\vec{L},t) = \sum_i U_{\alpha i}^* U_{\beta i} e^{i(\vec{p}_i^S\cdot\vec{L}-E_i(p_i^S)t)} G_i(\vec{L}-\vec{v}_{gi}t) \tag{34}$$

where

$$G_i(\vec{L}) = \int \mathrm{d}^3\vec{x}\, g_i^{D*}(\vec{x}) g_i^S(\vec{x}+\vec{L}) e^{i(\vec{p}_i^S-\vec{p}_i^D)\cdot\vec{x}}. \tag{35}$$

The exact moment of production or detection is usually not measured in neutrino experiments, so the probability of detecting the flavor β at the detector is given by the time integral

$$P(\nu_\alpha\to\nu_\beta;\vec{L}) = \int_{-\infty}^{\infty}\mathrm{d}t\left|\mathcal{A}_{\alpha\to\beta}(\vec{L},t)\right|^2. \tag{36}$$

Denoting $E_i = E_i(p_i^S)$ and defining

$$I_{ij}(\vec{L}) = \int_{-\infty}^{\infty}\mathrm{d}t G_j^*(\vec{L}-\vec{v}_{gj}t)G_i(\vec{L}-\vec{v}_{gi}t)e^{-i\Delta\phi_{ij}(\vec{L},t)} \tag{37}$$

with

$$\Delta\phi_{ij} = (E_i-E_j)t - (\vec{p}_i^S-\vec{p}_j^S)\cdot\vec{L}, \tag{38}$$

the probability becomes

$$P(\nu_\alpha\to\nu_\beta;\vec{L}) = \sum_{i,j} U_{\alpha i}^* U_{\beta i} U_{\alpha j} U_{\beta j}^* I_{ij}(\vec{L}). \tag{39}$$

The similarity of this formula to the standard formula for neutrino oscillations given in Eq. (9) is immediately noted and it will be further strengthened by the forms of $I_{ij}(\vec{L})$ obtained in Sections 3.3.3 and 3.4, which give the phase factor of the standard formula. The main phenomenon in neutrino oscillations is due to the phase factor $\Delta\phi_{ij}$, and it should be noted that its form in Eq. (38) is Lorentz invariant, removing the issue of Lorentz boosts invalidating the calculations.

The integral $I_{ij}(\vec{L})$ describes how much the wave packets of ith and jth massive neutrinos overlap, and is thus called an interference integral. For a discussion of why the interference integral $I_{ij}(\vec{L})$ and therefore the probability is Lorentz-invariant, see [17].

3.3.3 Calculating the interference integral

To get the probability (39) in a simpler form, the difference of momenta between produced and detected massive neutrino states is denoted by $\vec{\delta}_i = \vec{p}_i^S - \vec{p}_i^D$. With this and

$$\int \mathrm{d}^3\vec{x} e^{-i\vec{y}\cdot\vec{x}} = (2\pi)^3\delta^{(3)}(\vec{y}) \tag{40}$$

for the Dirac's delta function one may write

$$\begin{aligned} G_i(\vec{L}) &= \int \mathrm{d}^3\vec{x} g_i^{D*}(\vec{x}) g_i^S(\vec{x}+\vec{L}) e^{i(\vec{p}_i^S - \vec{p}_i^D)\cdot\vec{x}} \\ &= \int \mathrm{d}^3\vec{x} \int \frac{\mathrm{d}^3\vec{p}}{(2\pi)^{3/2}} \int \frac{\mathrm{d}^3\vec{q}}{(2\pi)^{3/2}} f_i^{D*}(\vec{p}) f_i^S(\vec{q}) \\ &\quad \times e^{-i\vec{p}\cdot\vec{x}} e^{i\vec{q}\cdot(\vec{x}+\vec{L})} e^{i\vec{\delta}_i\cdot\vec{x}} \\ &= \int \mathrm{d}^3\vec{p} \int \mathrm{d}^3\vec{q} \delta^{(3)}(\vec{p} - \vec{\delta}_i - \vec{q}) f_i^{D*}(\vec{p}) f_i^S(\vec{q}) e^{i\vec{q}\cdot\vec{L}} \\ &= \int \mathrm{d}^3\vec{q} f_i^{D*}(\vec{q}+\vec{\delta}_i) f_i^S(\vec{q}) e^{i\vec{q}\cdot\vec{L}}, \end{aligned} \tag{41}$$

where Eqs. (25), (29) and (35) have been used. This with the one-dimensional form of Eq. (40) leads to

$$\begin{aligned} I_{ij}(\vec{L}) = &\int_{-\infty}^{\infty} \mathrm{d}t \int \mathrm{d}^3\vec{p} f_j^D(\vec{p}+\vec{\delta}_j) f_j^{S*}(\vec{p}) e^{-i\vec{p}\cdot(\vec{L}-\vec{v}_{gj}t)} \\ &\times \int \mathrm{d}^3\vec{q} f_i^{D*}(\vec{q}+\vec{\delta}_i) f_i^S(\vec{q}) e^{i\vec{q}\cdot(\vec{L}-\vec{v}_{gi}t)} e^{-i((E_i-E_j)t - (\vec{p}_i^S - \vec{p}_j^S)\cdot\vec{L})} \\ = &2\pi \int \mathrm{d}^3\vec{p} \int \mathrm{d}^3\vec{q} f_j^D(\vec{p}+\vec{\delta}_j) f_j^{S*}(\vec{p}) f_i^{D*}(\vec{q}+\vec{\delta}_i) f_i^S(\vec{q}) \\ &\times \delta(\vec{q}\cdot\vec{v}_{gi} - \vec{p}\cdot\vec{v}_{gj} + \Delta E_{ij}) e^{i(\vec{q}-\vec{p}+\Delta\vec{p}_{ij}^S)\cdot\vec{L}}. \end{aligned} \tag{42}$$

To continue further, a choice of coordinates is made such that $\vec{v}_{gj} = \hat{z}v_{gj}$, where $\hat{z}$ is the unit vector in z-direction. The vector $\vec{p}$ is expressed as $\vec{p} = \vec{p}_{\parallel\hat{z}} + \vec{p}_{\perp\hat{z}}$ and others similarly. The following property is easily derived:

$$\int \mathrm{d}^3\vec{x} f(\vec{x}) \delta(\vec{x}\cdot z\hat{z} - a) = \frac{1}{z} \int \mathrm{d}^2\vec{x}_{\perp\hat{z}} f(\vec{x}_0 + \vec{x}_{\perp\hat{z}}), \tag{43}$$

where $\vec{x}_0$ is any vector such that $\vec{x}_0 \cdot z\hat{z} = a$ and f is a sufficiently smooth function. In the $\vec{p}$-integration of Eq. (42) one can choose $\vec{p}_0 = (\vec{q}\cdot\vec{v}_{gi} + \Delta E_{ij})\hat{z}/v_{gj}$, which clearly satisfies $\vec{p}_0 \cdot \hat{z}v_{gj} = \vec{q}\cdot\vec{v}_{gi} + \Delta E_{ij}$. Thus the eval-

uation of I_{ij} may be continued as

$$
\begin{aligned}
I_{ij}(\vec{L}) = & \frac{2\pi}{v_{gj}} \int \mathrm{d}^2\vec{p}_{\perp\hat{z}} \int \mathrm{d}^2\vec{q}_{\perp\hat{z}} \int \mathrm{d}\vec{q}_{\parallel\hat{z}} f_j^D \left(\vec{p}_{\perp\hat{z}} + (\vec{q}\cdot\vec{v}_{gi} + \Delta E_{ij}) \frac{\hat{z}}{v_{gj}} + \vec{\delta}_j \right) \\
& \times f_j^{S*} \left(\vec{p}_{\perp\hat{z}} + (\vec{q}\cdot\vec{v}_{gi} + \Delta E_{ij}) \frac{\hat{z}}{v_{gj}} \right) f_i^{D*}(\vec{q}_{\perp\hat{z}} + \vec{q}_{\parallel\hat{z}} + \vec{\delta}_i) \\
& \times f_i^S(\vec{q}_{\perp\hat{z}} + \vec{q}_{\parallel\hat{z}}) e^{i\left(\vec{q}_{\perp\hat{z}} + \vec{q}_{\parallel\hat{z}} - \left(\vec{p}_{\perp\hat{z}} + (\vec{q}\cdot\vec{v}_{gi} + \Delta E_{ij}) \frac{\hat{z}}{v_{gj}} \right) + \Delta\vec{p}_{ij}^S \right) \cdot \vec{L}} \\
= & \frac{2\pi}{v_{gj}} e^{i\left(\Delta\vec{p}_{ij}^S - \Delta E_{ij} \frac{\hat{z}}{v_{gj}} \right) \cdot \vec{L}} \int \mathrm{d}^2\vec{p}_{\perp\hat{z}} e^{-i\vec{p}_{\perp\hat{z}}\cdot\vec{L}} \\
& \times \int \mathrm{d}^2\vec{q}_{\perp\hat{z}} e^{i\left(\vec{q}_{\perp\hat{z}} - \vec{q}_{\perp\hat{z}}\cdot\vec{v}_{gi} \frac{\hat{z}}{v_{gj}} \right) \cdot \vec{L}} \int \mathrm{d}\vec{q}_{\parallel\hat{z}} e^{i\left(\vec{q}_{\parallel\hat{z}} - \vec{q}_{\parallel\hat{z}}\cdot\vec{v}_{gi} \frac{\hat{z}}{v_{gj}} \right) \cdot \vec{L}} \\
& \times f_j^D \left(\vec{p}_{\perp\hat{z}} + (\vec{q}\cdot\vec{v}_{gi} + \Delta E_{ij}) \frac{\hat{z}}{v_{gj}} + \vec{\delta}_j \right) f_i^{D*}(\vec{q} + \vec{\delta}_i) \\
& \times f_j^{S*} \left(\vec{p}_{\perp\hat{z}} + (\vec{q}\cdot\vec{v}_{gi} + \Delta E_{ij}) \frac{\hat{z}}{v_{gj}} \right) f_i^S(\vec{q}). \qquad (44)
\end{aligned}
$$

It is assumed that $\vec{v}_{gi} \parallel \vec{v}_{gj}$, that is $\vec{v}_{gi\perp\hat{z}} = 0$, which seems physically plausible. Under this assumption the phase factor in front of the integrals above becomes $(\Delta\vec{p}_{ij}^S - \Delta E_{ij}\hat{z}/v_{gj})\cdot\vec{L} = (\Delta p_{ij}^S - \Delta E_{ij}/v_{gj})\hat{z}\cdot\vec{L}$. To the first order in squared neutrino masses one may also approximate

$$
\begin{aligned}
\Delta E_{ij} = & E(p_i^S, m_i^2) - E(p_j^S, m_j^2) \\
\approx & \left. \frac{\partial E(p,m^2)}{\partial p} \right|_{p_j^S, m_j^2} (p_i^S - p_j^S) + \left. \frac{\partial E(p,m^2)}{\partial m^2} \right|_{p_j^S, m_j^2} (m_i^2 - m_j^2) \\
= & v_{gj}\Delta p_{ij}^S + \frac{1}{2E_j}\Delta m_{ij}^2, \qquad (45)
\end{aligned}
$$

where $E(p, m^2) = \sqrt{p^2 + m^2}$. Further noting that $p_j^S = v_{gj}E_j$, one obtains

$$
\begin{aligned}
I_{ij}(\vec{L}) = & \frac{2\pi}{v_{gj}} e^{-i\frac{\Delta m_{ij}^2}{2p}|\vec{L}_{\perp\hat{z}}|} \int \mathrm{d}^2\vec{p}_{\perp\hat{z}} e^{-i\vec{p}_{\perp\hat{z}}\cdot\vec{L}} \int \mathrm{d}^2\vec{q}_{\perp\hat{z}} e^{i\vec{q}_{\perp\hat{z}}\cdot\vec{L}} \\
& \times \int \mathrm{d}\vec{q}_{\parallel\hat{z}} e^{i\left(\vec{q}_{\parallel\hat{z}} - \vec{q}_{\parallel\hat{z}}\cdot\hat{z}\frac{v_{gi}}{v_{gj}}\hat{z} \right) \cdot \vec{L}} \\
& \times f_j^D \left(\vec{p}_{\perp\hat{z}} + (\vec{q}_{\parallel\hat{z}}\cdot\hat{z}v_{gi} + \Delta E_{ij}) \frac{\hat{z}}{v_{gj}} + \vec{\delta}_j \right) f_i^{D*}(\vec{q}_{\perp\hat{z}} + \vec{q}_{\parallel\hat{z}} + \vec{\delta}_i) \\
& \times f_j^{S*} \left(\vec{p}_{\perp\hat{z}} + (\vec{q}_{\parallel\hat{z}}\cdot\hat{z}v_{gi} + \Delta E_{ij}) \frac{\hat{z}}{v_{gj}} \right) f_i^S(\vec{q}_{\perp\hat{z}} + \vec{q}_{\parallel\hat{z}}), \qquad (46)
\end{aligned}
$$

where $p = p_j^S \approx \frac{1}{2}(p_i^S + p_j^S)$ (used only to divide Δm_{ij}^2 this approximation for p_j^S is valid to the first order in squared masses). It is rather convenient to

consider propagation in only one spatial dimension, which is a very good approximation when the distance between the production and detection of the neutrino is macroscopic [17]. Taking the one-dimensional version of Eq. (42) and carrying out the p-integration simplifies the previous equation to

$$I_{ij}(L) = \frac{2\pi}{v_{gj}} e^{-i\frac{\Delta m^2_{ij}}{2p}L} \int \mathrm{d}q e^{iq\left(1-\frac{v_{gi}}{v_{gj}}\right)L} f_j^D \left(q\frac{v_{gi}}{v_{gj}} + \frac{\Delta E_{ij}}{v_{gj}} + \delta_j\right) \times f_i^{D*}(q+\delta_i) f_j^{S*}\left(q\frac{v_{gi}}{v_{gj}} + \frac{\Delta E_{ij}}{v_{gj}}\right) f_i^S(q). \quad (47)$$

This calculation gives Eq. (39) a form very similar to that of Eq. (9).

The plane wave result of oscillation probabilities is obtained by letting $v_{gi}/v_{gj} \to 1$ and assuming that the shape factors become the same, i.e. $f_i^{S,D}(p) = f_j^{S,D}(p)$. See [17] for a description of how the latter assumptions follows from the former one. Using the normalization (50), the whole expression in Eq. (47) excluding the first phase factor tends to unity, leading to $I_{ij}(L) = \exp(-i\Delta m^2_{ij} L/2p)$. This is indeed the same formula obtained by using the plane wave approach.

3.3.4 Normalization

Different normalizations have been proposed for the momentum distribution functions f_i^S, for example [16]

$$\int \mathrm{d}p f_i^S(p) = \sqrt{2\pi}, \quad (48)$$

$$\int \mathrm{d}p \left|f_i^S(p)\right|^2 = 1, \quad (49)$$

and [17]

$$\int \mathrm{d}t \left|G_i(\vec{L} - \vec{v}_{gi}t)\right|^2 = 1. \quad (50)$$

Imposing such a normalization condition by hand is considered inconsistent. Instead, one should derive them from the temporal response function of the detector [17] or from a field theoretical treatment of the processes of neutrino creation, propagation and detection [19].

Fortunately, it is not entirely necessary dwell into the subtleties of normalization. Discussion of coherence, for example, does not require the calculation of any normalization factors. Also, in many applications one may normalize the probabilities themselves at the very end of the calculations without a need for a more explicit treatment. Terms of order $\mathcal{O}(m_\nu/E_\nu)$ can be neglected in the probabilities (but not the phase and coherence factors), because no detection apparatus has the accuracy to observe such subtle phenomena, and a misnormalization of this order is therefore rather insignificant.

3.4 Gaussian wave packets

It is usually assumed [17] that wave packets have a Gaussian form, e.g. in one dimension [16]

$$f_i^S(p) = \sqrt{\frac{1}{\sqrt{\pi}\sigma_{p_i}^S}} e^{-\frac{1}{2}((p-p_i^S)/\sigma_{p_i}^S)/2}. \tag{51}$$

If one defines "mean" group velocities as follows

$$v_{gij} = \frac{v_{gi}(\sigma_{p_i}^S)^2 + v_{gj}(\sigma_{p_j}^S)^2}{(\sigma_{p_i}^S)^2 + (\sigma_{p_j}^S)^2} \tag{52a}$$

$$v'_{gij} = \frac{(v_{gi}\sigma_{p_i}^S)^2 + (v_{gj}\sigma_{p_j}^S)^2}{v_{gi}(\sigma_{p_i}^S)^2 + v_{gj}(\sigma_{p_j}^S)^2} \tag{52b}$$

and assumes $p_i^S = p_i^D$, the interference integral $I_{ij}(L)$ turns out to be [16]

$$\begin{aligned} I_{ij}(L) = & \sqrt{\frac{2\eta_i\eta_j}{v_{gi}v_{gj}(\eta_i^2+\eta_j^2)}} \\ & \times \exp\left(-iL\left(\frac{\Delta m_{ij}^2}{p_i^S+p_j^S} - \frac{(v_{gi}^{-1}-v_{gj}^{-1})(E_i-E_j)(p_i^S\eta_i^2 - p_j^S\eta_j^2)}{(p_i^S+p_j^S)(\eta_i^2+\eta_j^2)}\right)\right) \\ & \times \exp\left(-\frac{(v_{gi}^{-1}-v_{gj}^{-1})^2L^2}{2(\eta_i^2+\eta_j^2)}\right) \exp\left(-\frac{(E_i-E_j)^2\eta_i^2\eta_j^2}{2(\eta_i^2+\eta_j^2)}\right), \end{aligned} \tag{53}$$

with $\eta_i = (v_{gi}\sigma_{p_i}^S)^{-1}$ in the notation used in Section 3.3.

This result contains essentially the same physics as the more general result in Eq. (47), as will be discussed shortly, but this more explicit form allows numerical treatment in Section 5, which cannot be done for generic wave packets.

4 Coherence

4.1 General remarks

In quantum mechanics the coherence of two states is essentially their ability to interfere. Fully coherent states can be described by a superposition of the states, and interference may take place. If the states are, instead, fully incoherent, there will be no interference. If the states are somehow spatially localized, overlap in the coordinate wave functions is necessary for coherence if the measurement process is spatially localized. A measurement that determines which of the states is in question destroys coherence — this happens in the double-slit experiment if the slit is determined and similarly in neutrino oscillations if the mass state is determined.

For two wave packets of massive neutrinos to be coherent they need to overlap significantly. If the wave packets have slightly different group velocities, they will slowly separate. When the wave packets become spatially too separated and thus incoherent, no more oscillations are observed. It must however be born in mind that these wave packets describe massive neutrinos, and thus have no well-defined flavor. Flavor measurement is therefore not deterministic even after coherence is lost, nor is it impossible to detect a change in flavor.

4.2 Coherence in plane wave approximation

Even the plane wave approach gives an opportunity to analyze coherence [7]. In the case of equal momentum oscillations are described by the angle $L\Delta m_{ij}^2/2p$. If the massive neutrinos are assumed to have a nonzero spread δp in momentum as any physical particle, there will also be spread in the oscillation angle. If this angular spread is of the order of 1, oscillations are washed out. The distance at which this washout happens is called the coherence length L_{ij}^{coh}, and it satisfies

$$\frac{L_{ij}^{\mathrm{coh}}\Delta m_{ij}^2}{2(p+\delta p)} \approx \frac{L_{ij}^{\mathrm{coh}}\Delta m_{ij}^2}{2p} - 1, \tag{54}$$

that is

$$L_{ij}^{\mathrm{coh}} \approx \frac{2p(p+\delta p)}{\delta p \Delta m_{ij}^2} \approx \frac{p}{\delta p}\frac{2p}{\Delta m_{ij}^2}. \tag{55}$$

When $L \gg L_{ij}^{\mathrm{coh}}$ the wash out is manifested by $\exp(-iL\Delta m_{ij}^2/2p) \approx \delta_{ij}$, giving the incoherent transition probability

$$P^{\mathrm{inc}}(\nu_\alpha \to \nu_\beta; L) \approx \sum_i |U_{\alpha i}U_{\beta i}|^2 . \tag{56}$$

That is, the probability no longer depends on the distance L, but has a constant value defined solely by the mixing matrix.

Similarly one can define the oscillation length $L_{ij}^{\mathrm{osc}} = 2p/\Delta m_{ij}^2$ describing the scale of the oscillations, using which the angle giving the oscillations is L/L_{ij}^{osc} and the coherence length is $L_{ij}^{\mathrm{coh}} = (p/\delta p)L_{ij}^{\mathrm{osc}}$.

Oscillation and coherence lengths defined this way may even be negative. Here only their absolute values are considered (implicitly), so that $L_{ij}^{\mathrm{osc,coh}} = L_{ji}^{\mathrm{osc,coh}}$.

The precise values of oscillation and coherence lengths have no specific meaning, since they only indicate the relevant length scales. Oscillations will be observable at lengths smaller than L^{osc}, but not if $L \ll L^{\mathrm{osc}}$, and similarly coherence will not be instantaneously lost at L^{coh}. Numerical examples in Section 5 will illustrate the relation between oscillation and oscillation length and also coherence and coherence length.

4.3 Coherence in wave packet treatment

In the wave packet approach coherence can be studied in terms of the interference integrals $I_{ij}(\vec{L})$ with $i \neq j$, as they are the source of oscillatory behavior in the system. Frequent use will be made of the Riemann–Lebesgue lemma, which can be stated as

$$\lim_{|\vec{x}|\to\infty} \int \mathrm{d}^n\vec{y} f(\vec{y}) e^{i\vec{x}\cdot\vec{y}} = 0 \tag{57}$$

for all smooth functions $f(\vec{y})$ that vanish when $|\vec{y}| \to \infty$. A mathematically more rigorous statement and treatment of this lemma is not needed here.

This lemma can immediately be applied to Eq. (46). The $\vec{p}_{\perp\hat{z}}$-integral vanishes if $\sigma_{\vec{p}_{j\perp\hat{z}}} L_{\perp\hat{z}} \gg 1$ and if $\sigma_{\vec{p}_{i\perp\hat{z}}} L_{\perp\hat{z}} \gg 1$, the same happens for the $\vec{q}_{\perp\hat{z}}$-integral. Here $\sigma_{\vec{p}_{i\perp\hat{z}}}$ is an effective wave packet spread in momentum space combining $\sigma^S_{\vec{p}_{i\perp\hat{z}}}$ and $\sigma^D_{\vec{p}_{i\perp\hat{z}}}$. In case of Gaussian wave packets $\sigma_{\vec{p}_{i\perp\hat{z}}} = \sqrt{(\sigma^S_{\vec{p}_{i\perp\hat{z}}})^2 + (\sigma^D_{\vec{p}_{i\perp\hat{z}}})^2}$ [17].

As noted in Section 3.3.1, wave packets have constant shape. By Heisenberg's uncertainty principle, $\sigma_{\vec{p}_{i\perp\hat{z}}} L_{\perp\hat{z}} \gg 1$ is equivalent to $L_{\perp\hat{z}} \gg \sigma_{\vec{x}_{i\perp\hat{z}}}$. Thus for coherence the wave packet width perpendicular to the direction of propagation must not be too much smaller than the distance of the detector from the path of the wave packet. This is merely a requirement that the neutrinos must not miss the detector, and it is easily achieved by placing the detector in such a position (or equivalently, aiming the beam) that $\vec{L} \parallel \hat{z}$.

Should this condition not be met, $I_{ij}(\vec{L})$ will tend to zero even for $i = j$, so the condition in question is not one of coherence but of general detectability of the produced neutrino. It should be noted that the suppression of the interference integral in the case of ill-placed detector is counter-acted by the normalization (50) so that little or no change takes place in the probabilities. However, this normalization tries to ensure that the sum of the three flavor detection probabilities is unity, whereas the total detection probability will obviously decrease if the detector does not lie on the neutrino path. The above discussion in terms of suppression of $I_{ij}(\vec{L})$ can be viewed as a hint arising from wave packet treatment suggesting that neutrinos should hit the detector.

Given this requirement of not missing the detector, one may neglect directions perpendicular to $\hat{z}$ and use the one-dimensional Eq. (47). The q-integral will vanish if $\sigma_p \left|1 - v_{gi}/v_{gj}\right| L \gg 1$, where $\sigma_p = \min\{\sigma_{p_i}, \sigma_{p_j}\}$. Denoting $\Delta v_{gij} = |v_{gi} - v_{gj}|$, this can be restated as $L \gg L^{\mathrm{coh}}_{ij} = v_g/(\sigma_p \Delta v_{gij})$. This is a condition for significant wave packet separation [17], and can easily be understood to be so in terms of classical kinematics. When $L \ll L^{\mathrm{coh}}_{ij}$, the wave packets are coherent and the value of the integral is practically independent of L.

Assuming that $\sigma_{p_i} = \sigma_{p_j}$ and either $E_i = E_j = E$ or $p^S_i = p^S_j = p$ gives $v_{gi} - v_{gj} \approx -\Delta m^2_{ij}/2E^2$ or $v_{gi} - v_{gj} \approx -\Delta m^2_{ij}/2p^2$, respectively. Since

coherence length is uninteresting in very high accuracy, one can use $E \approx p$ and $v_g \approx 1$ to see that in both cases $L_{ij}^{\mathrm{coh}} \approx (p/\sigma_p)(2p/\Delta m_{ij}^2)$. This is exactly the result that was obtained in terms of plane waves and uncertainty.

Other conditions for non-vanishing $I_{ij}(\vec{L})$ are found by demanding that the functions in the integral overlap sufficiently well. All the shape functions $f_{i,j}^{S,D}$ Eq. (47) are strongly peaked at the origin, whence in order to have significant overlap the quantities δ_i, δ_j, and $\Delta E_{ij}/v_{gj}$ have to be sufficiently small in comparison to the widths of the shape functions.

For the first two one may demand that $\delta_i \ll \sigma_{p_i}^S$ or $\delta_j \ll \sigma_{p_j}^S$. This is nothing but approximate momentum conservation in the process, and comes therefore as no surprise. Similarly to neutrinos not missing the detector, this is an obvious requirement. The interesting thing is that neither of these need be imposed by hand, since they follow from a careful wave packet treatment.

The remaining requirement for coherence is $\Delta E_{ij}/v_{gj} \ll \sigma_p$. For a particle on its mass shell[3], $E^2 = m^2 + p^2$. Differentiating this relation gives

$$E\sigma_E = p\sigma_p, \tag{58}$$

where σ_E and σ_p is the uncertainties of energy and momentum of the produced neutrino, and thus $v_{gj}\sigma_p \approx \sigma_E$. This gives the coherence condition a simple form in terms of energy only: $\Delta E_{ij} \ll \sigma_E$.

This has a physical meaning giving a crucial requirement not for the relative position of the detector from the source but for the production and detection processes. Should the opposite inequality $\Delta E_{ij} \gg \sigma_E$ hold, the energy of the system could be measured accurately enough to determine which *mass* eigenstate is in question. In such a situation the neutrino is composed of a single mass eigenstate and no oscillations will take place. Also, the produced neutrino will not have a well-defined flavor.

Unless $\Delta m_{ij}^2/2E\sigma_E \approx v_g \left|\Delta p\right|/\sigma_E \gg 1$ as would be the case for Mössbauer neutrino experiments [20, 21], $\Delta E_{ij} \gg \sigma_E$ also guarantees that $\Delta p_{ij} \gg \sigma_p$, as shown in [17]. This is similarly required in order to not have a definite mass state. Thus $\Delta E_{ij} \gg \sigma_E$ or equivalently $\Delta E_{ij}/v_{gj} \ll \sigma_p$ ensures that the production and detection processes are suited for coherent neutrinos.

4.4 Restoration of coherence at detection

A possibility of coherent detection remains even if the wave packets have separated so that the massive neutrinos are incoherent. If the neutrino detector has a high energy resolution, its time resolution is inevitably low. This may give enough time for two or more incoherent mass states to interact with the detector, causing the wave packets being observed coherently. [17]

[3]Neutrinos can be considered on-shell after traveling a distance x from the production site such that $px \gg 1$. Also, since each mass state is on-shell and they have approximately the same energy and momentum, their superposition also fulfills the energy-momentum relation of an on-shell particle. [17]

If the momentum uncertainties σ_p above are effective uncertainties combining the uncertainties of production and detection processes, the possibility of restoration of coherence is already taken into account. It is therefore important to consider both production and detection processes when estimating the wave packet width in either momentum or coordinate representation.

4.5 Wave packet spreading

Even if wave packets get separated by more than the initial size of the wave packets, coherence may remain if wave packets spread to still overlap each other. The spreading of wave packets is a common phenomenon in all quantum mechanics, and its effect on coherent neutrino propagation needs to be discussed.

Eq. (19) of the Section 3.2 gives the time evolution of the wave packet length σ_x:

$$\sigma_x(t) = \sigma_{x0}\sqrt{1 + \frac{\sigma_p^4 t^2 v^2 (1-v^2)^2}{p^2}}. \tag{59}$$

Using $1 - v^2 = (m_\nu/E)^2 \approx (m_\nu/p)^2$, $\Delta p_{ij} \approx \Delta m_{ij}^2/2p$, and $t \approx L_{ij}^{\mathrm{coh}}$, one obtains

$$\frac{\sigma_p^2 t v (1-v^2)}{p} \approx \left(\frac{m_\nu}{p}\right)^2 \frac{\sigma_p}{\Delta p_{ij}}. \tag{60}$$

For coherently produced ultrarelativistic neutrinos $m_\nu \ll p$ and $\sigma_p \gtrsim \Delta p_{ij}$. Assuming $\sigma_p/\Delta p_{ij} \ll (p/m_\nu)^2$ yields $\sigma_x(L_{ij}^{\mathrm{coh}}) \approx \sigma_{x0}$, so the wave packet spreading is insignificant for the loss of coherence.

4.6 The case of high flux

If the flux of produced neutrinos is high enough, the wave packets from different production processes may begin to overlap. Assuming that the neutrino beam is directed (no neutrino has velocity components perpendicular to other neutrino velocities), this overlap will not be lost at any distance. It might be that the flavor detection probabilities become the incoherent probabilities of Eq. (56) in such a case, but it seems also possible that the probabilities are unchanged from standard ones.

To find the flux scale at which such an overlap becomes significant, it is assumed that neutrinos are produced in a rectangular box with one face facing the direction of the detector. The length of the edges perpendicular to this face is h. An emitted neutrino is considered to be a box of length $\sigma_{x\parallel}$ and width (to both directions perpendicular to the line to the detector) $\sigma_{x\perp}$. The detector is assumed to be far away in comparison to the widths of the neutrino source and detector, so that all observable neutrinos have parallel velocities. Therefore only neutrinos heading towards the detector are considered.

Let a neutrino be produced at a distance $\tilde{h}$ from the face of the source heading the detector and head towards the detector at approximately light speed. When it has traveled the length l, it has swept approximately the volume $\min\{\tilde{h}, l\}\sigma_{x\perp}^2$. If the neutrino flux density is J, there are J/h reactions per unit time and cubed unit length in the source, and thus the number of neutrinos produced this swept volume is $\min\{\tilde{h}, l\}\sigma_{x\perp}^2 lJ/h$.

To see when the next neutrino — a neutrino with parallel velocity and trajectories close enough to allow overlap — is produced, this number is set to one. The corresponding value of l is denoted by l_1. In the case of high flux $l_1 \lesssim \sigma_{x\parallel}$. In a physical application the length $\sigma_{x\parallel}$ of the wave packet can be at most in the scale of interatomic distances in the source, whereas the thickness h of the source is numerous interatomic distances. Because $\tilde{h} \sim h$ for most neutrinos, it is assumed that $l_1 < h$.

Under this assumption one obtains the equation $l_1^2\sigma_{x\perp}^2 J/h \approx 1$ for l_1, which yields $l_1 \approx \sqrt{h/J}/\sigma_{x\perp}$. Using $l_1 \lesssim \sigma_{x\parallel}$ with this result gives the condition

$$J(\sigma_{x\perp}\sigma_{x\parallel})^2 \gtrsim h \tag{61}$$

for high flux. If, on the other hand, $J(\sigma_{x\perp}\sigma_{x\parallel})^2 \ll h$, the neutrino density is so low that no significant overlap between wave packets originating from different source processes takes place.

It must be noted, however, that such a high flux effect on neutrino production will only be significant if the overlapping neutrinos originating from different production processes are coherent. This requires that the source of neutrinos is — to some extent at least — a macroscopic coherent quantum state. It is unclear whether such a situation is possible or not. The most prominent possibility for such a phenomenon is the Mössbauer neutrino experiment, where the entire lattice could act as a single state.

4.7 Summary

The previous analysis revealed several conditions for coherent neutrino oscillation (for a discussion and an explanation of the symbols used, see the corresponding sections):

1. The produced neutrinos are ultrarelativistic. All calculations are based on this assumption, and also a neutrino can only be detected with current detectors if $E_\nu \gg 1000 m_\nu$.

2. Neutrinos must hit the detector (Section 4.3). This condition is trivial, but does arise from the wave packet treatment.

3. Neutrinos must not travel too long distances (Sections 4.2, 4.3 and 4.4). The requirement can be stated as $L \ll L_{ij}^{\mathrm{coh}} = (p/\sigma_p)(2p/\Delta m_{ij}^2)$.

4. The energy and momentum uncertainties must exceed the energy and momentum differences between massive neutrinos (Section 4.3). Otherwise the detector could be able to measure which mass state is detected.

5. Wave packets can spread to counteract separation (Section 4.5). Spread is negligibly small if $\sigma_p/\Delta p_{ij} \ll (p/m_\nu)^2$. This condition seems to be easily satisfied and is equivalent to $(\sigma_p/p)(2m_\nu^2/\Delta m_{ij}^2) \ll 1$.

6. Neutrino flux must not be too high (Section 4.6). The neutrino flux density J must fulfill $J(\sigma_{x\perp}\sigma_{x\parallel})^2 \ll h$ in order to remain in the low flux regime, or the neutrino production must be incoherent. Whether or not observable phenomena take place if the flux is higher is unclear.

Whether or not these conditions are or can be met in future experiments will be discussed in Section 6.

5 Numerical analysis

5.1 Preliminary assumptions and mixing parameters

In order to carry out numerical analysis, several assumptions have to be made. The wave packets are assumed to be Gaussian as in Section 3.4, and their momenta and momentum uncertainties are assumed to coincide, i.e. $p_i^S = p_i^D = p$ and $\sigma_{p_i} = \sigma_p$ for all i. The notation follows that of Sections 3.3 and 3.4.

Doing calculations to the first order in squared neutrino mass differences, one finds

$$E_i - E_j \approx p + \frac{m_i^2}{2p} - p - \frac{m_j^2}{2p} = \frac{\Delta m_{ij}^2}{2p}, \tag{62a}$$

$$v_{gi}^{-1} - v_{gj}^{-1} = \frac{E_i}{p} - \frac{E_j}{p} \approx \frac{\Delta m_{ij}^2}{2p^2}, \tag{62b}$$

$$p\eta_i^2 - p\eta_j^2 = \frac{E_i^2}{p\sigma_p^2} - \frac{E_j^2}{p\sigma_p^2} = \frac{1}{p\sigma_p^2}(p^2 + m_i^2 - p^2 - m_j^2) = \frac{\Delta m_{ij}^2}{p\sigma_p^2}. \tag{62c}$$

It is assumed that $v_{gi} \approx v_{gi} \approx 1$ everywhere where their difference is not needed, and similarly $\eta_i \approx \eta_j$, which gives $\eta_i \approx \sigma_p^{-1}$.

Under these assumptions Eq. (53) simplifies to

$$
\begin{aligned}
I_{ij}(L) &\approx \exp\left(-iL\left(\frac{\Delta m_{ij}^2}{2p} - \frac{\frac{\Delta m_{ij}^2}{2p^2}\frac{\Delta m_{ij}^2}{2p}\frac{\Delta m_{ij}^2}{p\sigma_p^2}}{2p\cdot\eta^2}\right)\right) \\
&\quad\times \exp\left(-\frac{\left(\frac{\Delta m_{ij}^2}{2p^2}\right)^2 L^2}{4\eta^2}\right)\exp\left(-\frac{\left(\frac{\Delta m_{ij}^2}{2p}\right)^2\eta^2}{4}\right) \\
&\approx \exp\left(-i\frac{L\Delta m_{ij}^2}{2p}\right)\exp\left(-\left(\frac{L\sigma_p\Delta m_{ij}^2}{4p^2}\right)^2 - \left(\frac{\Delta m_{ij}^2}{4p^2\sigma_p}\right)^2\right). \qquad (63)
\end{aligned}
$$

At short distances, when wave packets are still coherent, the probability only depends on the ratio L/p. The L- and p-dependence of decoherence phenomena (described here by the exponential function with real argument) cannot be described in terms of the ratio. The reason for the suppression of coherence phenomena at short distances is the smallness of the coefficients of L and p in the latter exponential function.

In the following the momentum is given the value $p = 4$ MeV, where the reactor neutrino event rate approximately peaks and which is also suitable for detection of electron neutrinos via inverse beta decay [22, 23, 24]. Assuming that neutrinos can be localized in production and detection processes to the atomic distance scale [22], the effective position uncertainty is $\sigma_x \sim 1$ nm. By the uncertainty principle the momentum uncertainty can be approximated, and is given the numerical value $\sigma_p = 200$ eV in the present analysis.

The mixing matrix U is conventionally parametrized by angles θ_{12}, θ_{13}, θ_{23}, α_1, α_2, and δ so that [25]

$$
\begin{aligned}
U = &\begin{bmatrix} 1 & 0 & 0 \\ 0 & c_{23} & s_{23} \\ 0 & -s_{23} & c_{23} \end{bmatrix}\begin{bmatrix} c_{13} & 0 & s_{13}e^{-i\delta} \\ 0 & 1 & 0 \\ -s_{13}e^{i\delta} & 0 & c_{13} \end{bmatrix} \\
&\times\begin{bmatrix} c_{13} & s_{13} & 0 \\ -s_{13} & c_{13} & 0 \\ 0 & 0 & 1 \end{bmatrix}\begin{bmatrix} e^{i\alpha_1/2} & 0 & 0 \\ 0 & e^{i\alpha_2/2} & 0 \\ 0 & 0 & 1 \end{bmatrix}, \qquad (64)
\end{aligned}
$$

where the trigonometric functions have been abbreviated as $c_{ij} = \cos\theta_{ij}$ and $s_{ij} = \sin\theta_{ij}$. The angles θ_{ij} describe the strength of mixing between the ith and jth mass states. The Dirac phase δ is the only physically meaningful phase if neutrinos are Dirac particles, but if neutrinos are Majorana particles instead, the Majorana angles α_1 and α_2 are also have a physical significance.

For numerical calculations the following values are chosen, based on the

experimental limits [26]:

$$\theta_{12} = 0.600967 \tag{65a}$$
$$\theta_{23} = 0.714450 \tag{65b}$$
$$\theta_{13} = 0.100000 \tag{65c}$$
$$\Delta m^2_{21} = 7.59 \cdot 10^{-5}\ \text{eV}^2 \tag{65d}$$
$$\Delta m^2_{32} = 243.00 \cdot 10^{-5}\ \text{eV}^2 \tag{65e}$$
$$\Delta m^2_{31} = 250.59 \cdot 10^{-5}\ \text{eV}^2. \tag{65f}$$

With these values one may estimate that

$$\frac{\sigma_p}{\Delta_{31} p} \approx \frac{2p\sigma_p}{\Delta m^2_{31}} \approx 6 \cdot 10^{11} \gg 1, \tag{66}$$

and similarly the condition $\sigma_E/\Delta_{31}E \gg 1$ of Section 4.3 is fulfilled, so that the massive neutrinos are indeed produced coherently.

5.2 Neutrino oscillations on different scales

With the parameter values of the previous section, i.e. $p = 4$ MeV and mixing angles and squared mass differences given by Eqs. (65a)–(65f), transition probabilities may be given numerical values as a function of L. To get an estimate of length scales to investigate, the oscillation and coherence lengths $L^{\text{osc}}_{ij} = 2p/\Delta m^2_{ij}$ and $L^{\text{coh}}_{ij} = (p/\sigma_p)(2p/\Delta m^2_{ij})$ are calculated:

$$L^{\text{osc}}_{12} \approx 20.806\ \text{km} \tag{67a}$$
$$L^{\text{osc}}_{13} \approx 0.63\ \text{km} \tag{67b}$$
$$L^{\text{osc}}_{23} \approx 0.65\ \text{km} \tag{67c}$$
$$L^{\text{coh}}_{12} \approx 416000\ \text{km} \tag{67d}$$
$$L^{\text{coh}}_{13} \approx 12600\ \text{km} \tag{67e}$$
$$L^{\text{coh}}_{23} \approx 13000\ \text{km}. \tag{67f}$$

The transition probabilities for different flavor neutrinos when an electron neutrino is produced is plotted in Fig. 1 on various length scales of interest. Fig. 1a shows how the oscillations behave at short length scales and also implies that at very short scales (say, $L \sim 1$ m) practically no oscillations are observed.

Fig. 1b demonstrates the oscillations at a slightly larger scale, revealing another level of oscillations. The period of the shorter scale oscillations is $2\pi L^{\text{osc}}_{13} \approx 2\pi L^{\text{osc}}_{23} \approx 4$ km, whereas that of the longer scale oscillations is $2\pi L^{\text{osc}}_{12} \approx 130$ km, as can be seen in the figure.

The last two plots in Fig. 1 demonstrate the loss of coherence. The oscillation lengths are much smaller than the length scale plotted, wherefore

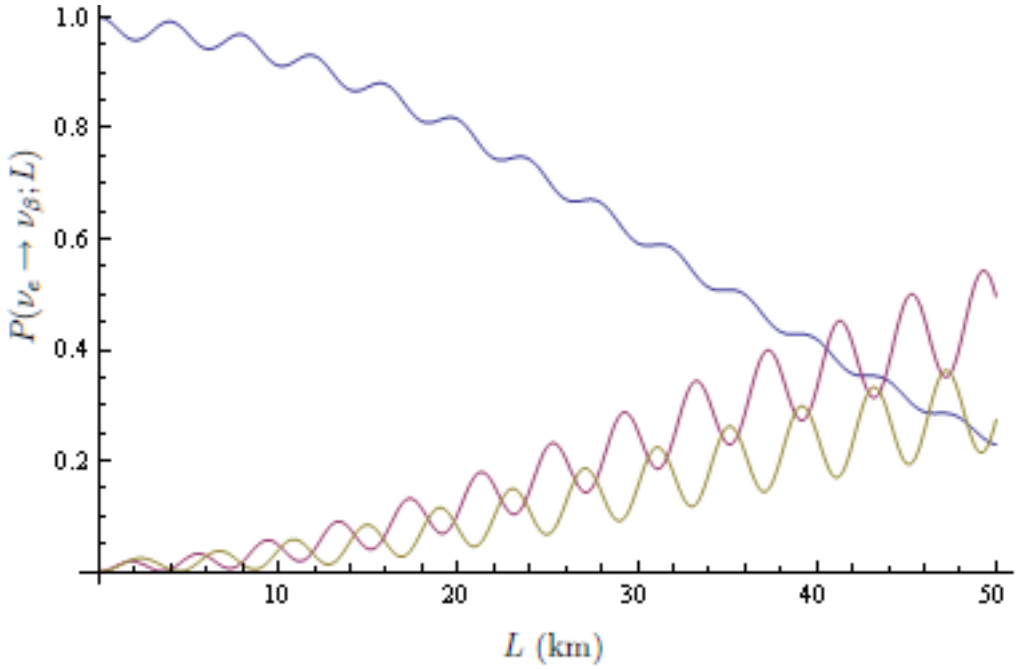
1.0
0.8
0.6
0.4
0.2
$P(\nu_e \to \nu_\beta; L)$
10
20
30
40
50
L (km)

(a)

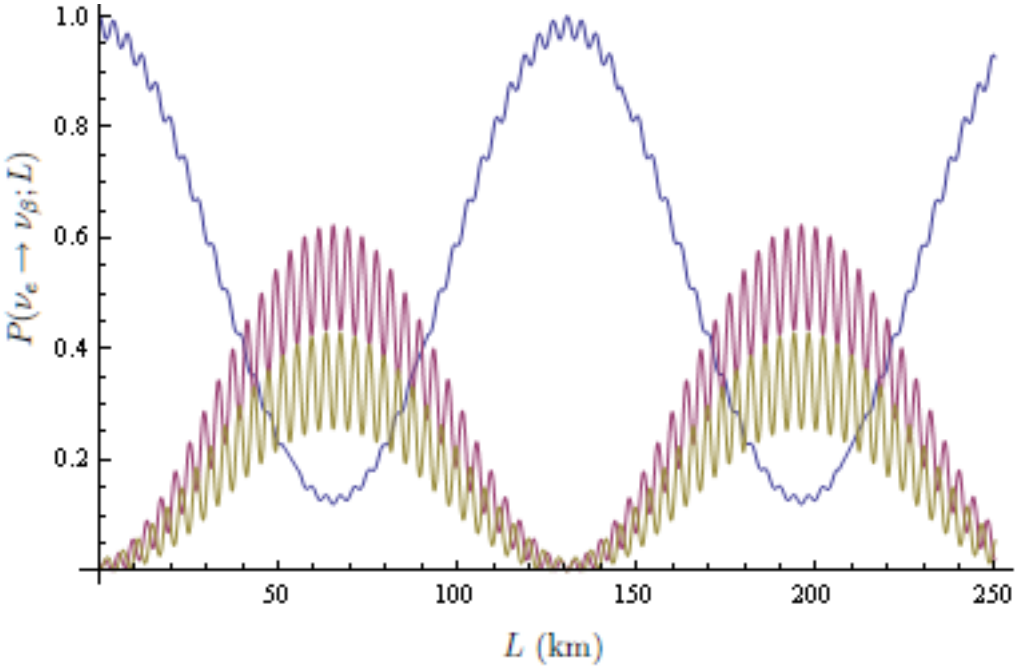
1.0
0.8
0.6
0.4
0.2
$P(\nu_e \to \nu_\beta; L)$
50
100
150
200
250
L (km)

(b)

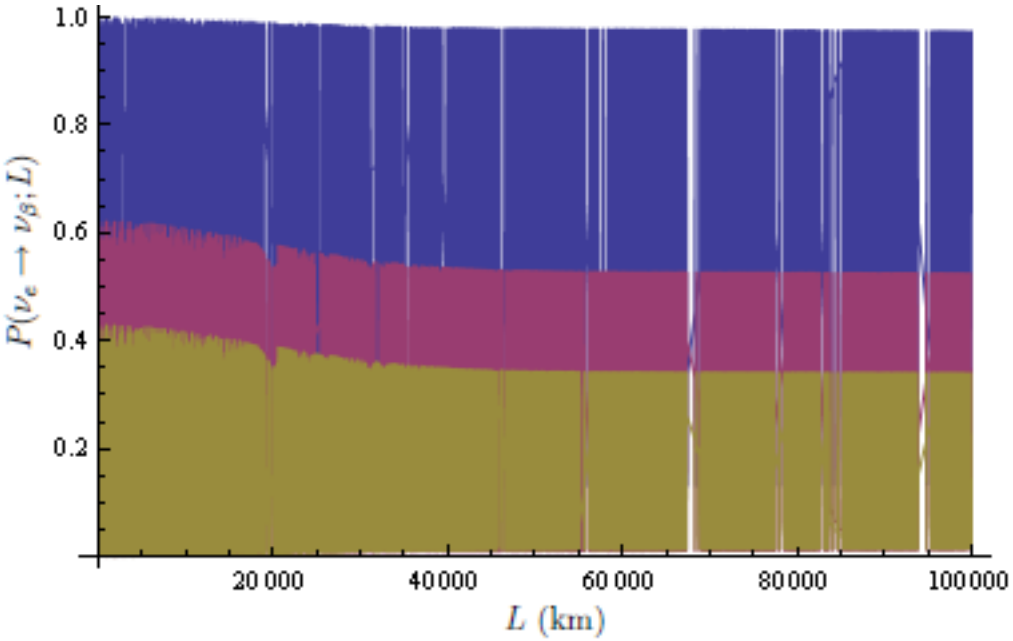

(c)

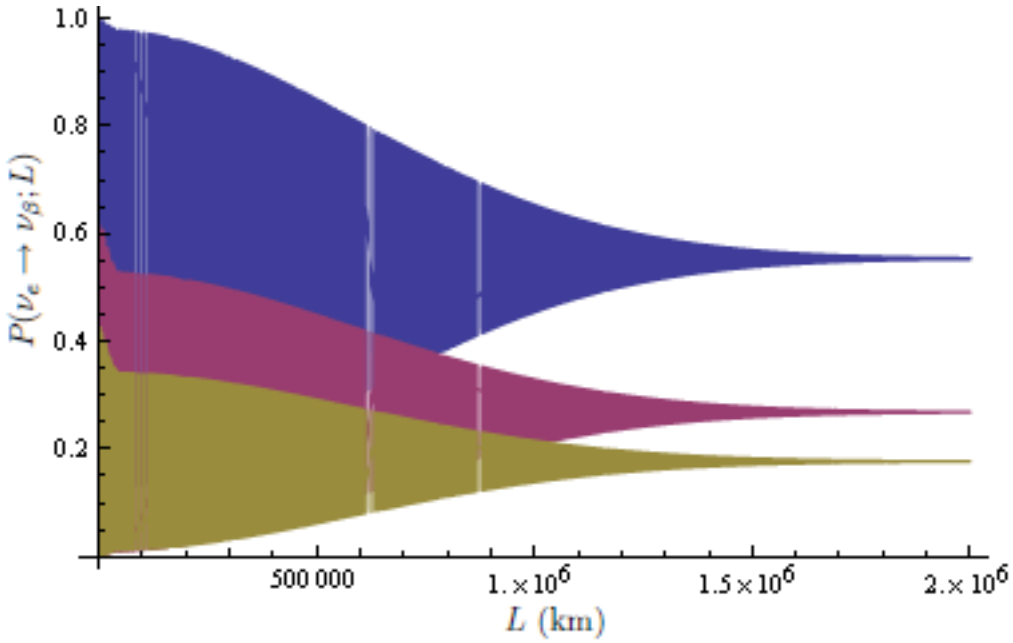

(d)

Figure 1: Probabilities for detecting electron, muon, and tau neutrinos (blue, purple, and brown lines, respectively) as a function of distance L when an electron neutrino is originally produced at distance scales of (a) 50 km, (b) 250 km, (c) $1 \cdot 10^5$ km, and (d) $2 \cdot 10^6$ km.

the oscillation pattern is not visible. In Fig. 1c one may see a small decrease in the amplitude of probability oscillations caused by the wave packet of the heaviest massive neutrino ν_3 being separated from those of the lighter ones (that is, $I_{i3}(L) \to 0$ in Eq. (63) for $i = 1, 2$).

A much more significant change in the probability pattern is visible in Fig. 1d. All wave packets are separated from each other, and all oscillations are lost. The chance of flavor change remains, and is indeed significant.

As Figs. 1c and 1d show, only the amplitudes of the oscillations in probability are of interest at large distance scales, because the length scale greatly exceeds that of the oscillations. Thus a simpler framework for the analysis of loss of coherence may be obtained through the analysis of envelope curves to the flavor probability curves.

Because it was assumed that $\delta = \alpha_1 = \alpha_2 = 0$, U is real, and the transition probability given in Eqs. (39) and (63) becomes

$$\begin{aligned} P(\nu_\alpha \to \nu_\beta; L) &= \sum_{i,j} U_{\alpha i} U_{\beta i} U_{\alpha j} U_{\beta j} e^{i\varphi_{ij}} C_{ij} \\ &= \sum_i (U_{\alpha i} U_{\beta i})^2 + 2 \sum_{i<j} U_{\alpha i} U_{\beta i} U_{\alpha j} U_{\beta j} \cos(\varphi_{ij}) C_{ij} \end{aligned} \tag{68}$$

with abbreviating notations $\varphi_{ij} = -L\Delta m_{ij}^2/2p$ and

$$C_{ij} = \exp\left(- \left(\frac{L\sigma_p \Delta m_{ij}^2}{4p^2} \right)^2 - \left(\frac{\Delta m_{ij}^2}{4p^2 \sigma_p} \right)^2 \right). \tag{69}$$

Using $-1 \le \cos(\varphi_{ij}) \le 1$ one immediately obtains upper and lower bounds for the transition probabilities:

$$P^{\text{up}}(\nu_\alpha \to \nu_\beta; L) = \sum_i (U_{\alpha i} U_{\beta i})^2 + 2 \sum_{i<j} |U_{\alpha i} U_{\beta i} U_{\alpha j} U_{\beta j}| \, C_{ij}, \tag{70a}$$

$$P^{\text{low}}(\nu_\alpha \to \nu_\beta; L) = \sum_i (U_{\alpha i} U_{\beta i})^2 - 2 \sum_{i<j} |U_{\alpha i} U_{\beta i} U_{\alpha j} U_{\beta j}| \, C_{ij}. \tag{70b}$$

The area between these curves is shown shaded in Fig. 2. Comparison of Figs. 1d and 2 indicates that these bounds indeed give the envelope curves of transition probablities except at small L, where the lower bound may be negative. The first term in the envelope functions above is simply the incoherent transition probability of Eq. (56).

For comparison, the behavior of the probabilities when a muon neutrino is produced is plotted in Fig. 3. The pattern is distinguishable from that of the electron neutrino, but very similar in its structure.

6 Coherence in future experiments

The coherence length for the ith and jth mass state given by Eq. (56) (obtained for both plane waves and wave packets in Sections 4.2 and 4.3) was

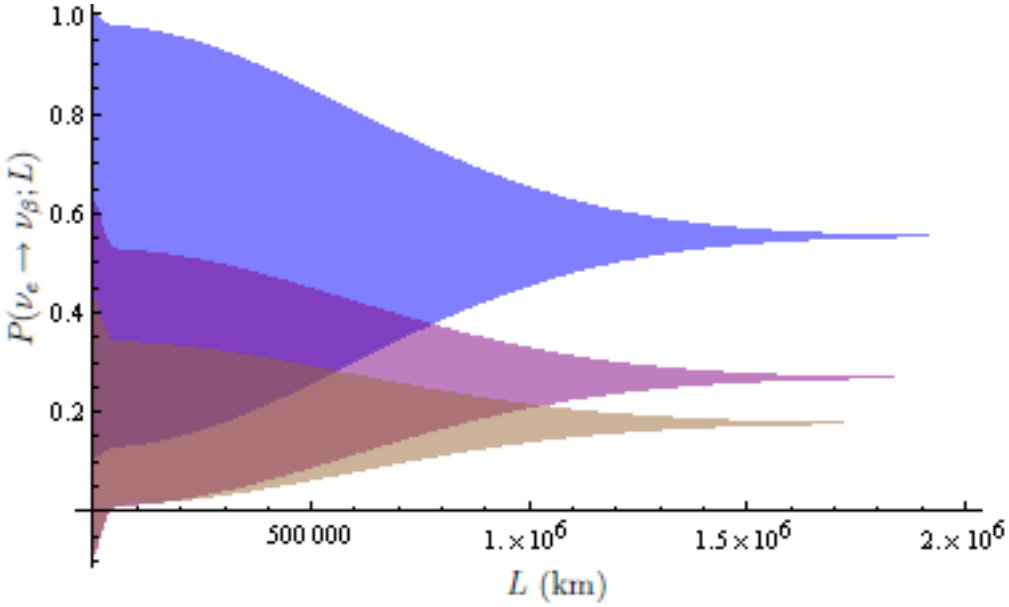

Figure 2: Upper and lower bounds — the oscillation envelopes — for probabilities for detecting electron, muon, and tau neutrinos (blue, purple, and brown shaded areas respectively) as a function of distance L at $2 \cdot 10^6$ km range when an electron neutrino is originally produced.

$L_{ij}^{\mathrm{coh}} = 2E^2\sigma_x/\Delta m_{ij}^2$ (with the approximations $\sigma_x\sigma_p \approx 1$ and $p \approx E$). For convenience, this can be written in the form

$$L_{ij}^{\mathrm{coh}} = 2 \cdot 10^5 \text{ km} \left(\frac{E}{\text{MeV}}\right)^2 \left(\frac{\sigma_x}{10^{-9} \text{ m}}\right) \left(\frac{\Delta m_{ij}^2}{10^{-5} \text{ eV}^2}\right)^{-1}. \tag{71}$$

Using $\Delta m_{21}^2 = 7.59 \cdot 10^{-5}$ eV^2 and $E = 4$ MeV as in Section 5.1 and estimating $\sigma_x = 10^{-11}$ m [22], one obtains the coherence length $L_{21}^{\mathrm{coh}} \approx 4200$ km, which is a feasible distance for oscillation experiments on Earth. If the wave packet size is one order of magnitude larger than estimated here, incoherence is beyond reach in any terrestrial experiment.

The solar neutrinos have smaller energy than those produced in reactors, although roughly of the same order of magnitude. If their wave packet sizes are anywhere near the nanometer scale or smaller, the neutrinos observed on Earth are incoherent. Coherent detection is possible, however, if the time resolution of the measurement device is low enough (as can be caused by high energy resolution), as was discussed in Section 4.4.

A condition for high flux, Eq. (61), was derived in Section 4.6. In the case of high flux neutrino wave packets originating from different production processes within the source overlap. If one assumes that the length of the neutrino wave packet is equal to its width, $\sigma_{x\perp} = \sigma_{x\parallel} = \sigma_x$, then the low

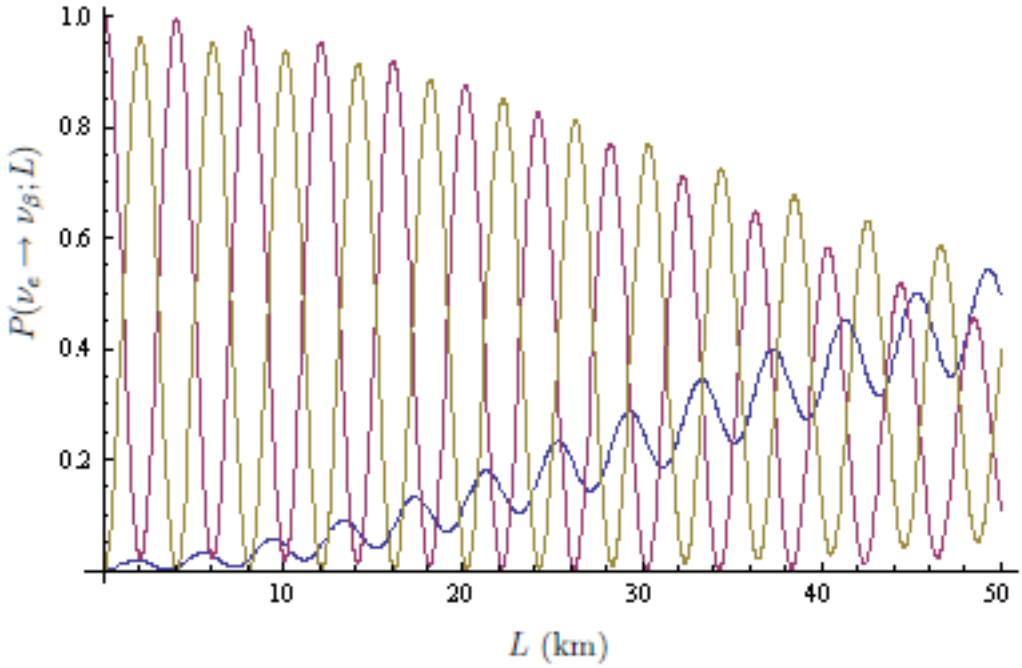

(a)

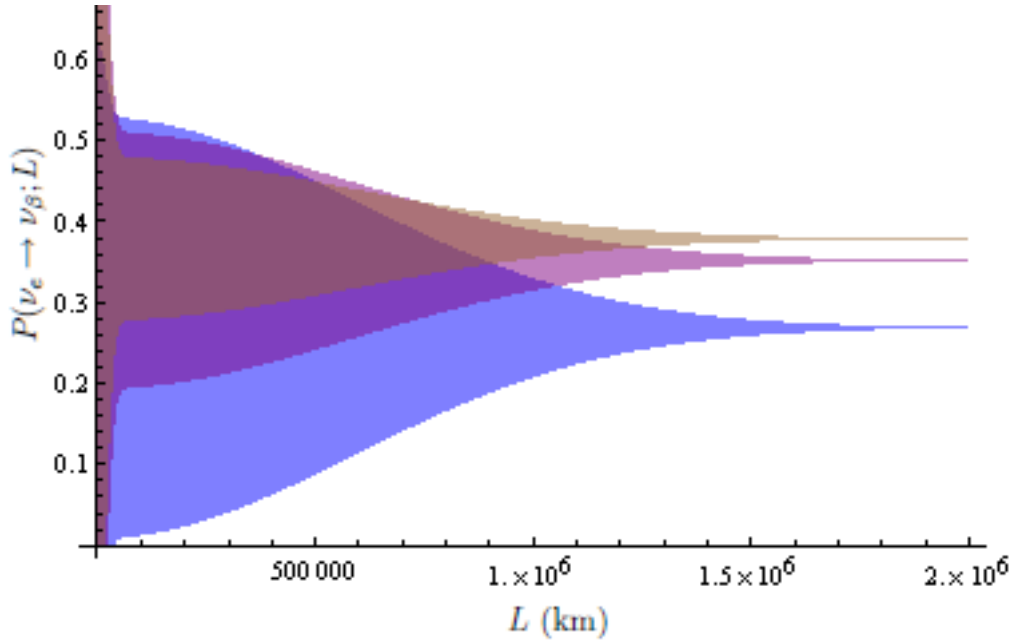

(b)

Figure 3: Probabilities for detecting electron, muon, and tau neutrinos (blue, purple, and brown lines and shaded areas respectively) as a function of distance L when a muon neutrino is originally produced at distance scales of (a) 50 km and (b) $2 \cdot 10^6$ km.

flux condition may be written as $\sigma_x \ll \sigma_{\max}$, where the limit wave packet size is $\sigma_{\max} = (h/J)^{1/4}$. For high flux phenomena to take place, the different neutrinos should be produced coherently, which requires that the source is a macroscopic coherent quantum state. The Sun or a nuclear reactor do not meet this condition, but their wave packet sizes are compared to the one required for high flux to give an insight to the order of magnitude of the high flux requirement.

For solar neutrinos the flux is approximately $J = 6 \cdot 10^{10}\ \mathrm{cm}^{-2}\mathrm{s}^{-1}$ [27], and the depth h of the source is estimated to be twice the radius of the solar core, $h = 0.5 R_\odot$ [28]. With these values one obtains $\sigma_{\max} \approx 4$ m. Since the wave packet size is usually assumed to be at most in the nanometer scale, the solar neutrino flux is low.

The flux of neutrinos from a nuclear reactor are of the order of $J = 6 \cdot 10^{12}\ \mathrm{cm}^{-2}\mathrm{s}^{-1}$ [29], and a the reactor size is estimated to be $h = 1$ m. These estimates give the wave packet size the upper limit $\sigma_{\max} \approx 8$ mm, so the neutrinos are again safely in the low flux regime.

The neutrino fluxes from these sources are so many orders of magnitude lower than would be required high flux that it seems unlikely to be able to experimentally verify the existence or nonexistence of any possible high flux phenomena in near future. Whether or not such a high flux would have an impact on neutrino oscillation can only be analyzed theoretically unless unexpectedly great experimental advancements are made.

References

[1] J. Barranco, A. Bolanos, O. G. Miranda, C. A. Moura, and T. I. Rashba. Neutrino phenomenology and unparticle physics. *ArXiv e-prints*, November 2009.

[2] J. N. Abdurashitov et al. Measurement of the solar neutrino capture rate by the Russian-American gallium solar neutrino experiment during one half of the 22-year cycle of solar activity. *J. Exp. Theor. Phys.*, 95:181–193, 2002.

[3] Francesco Vissani, Giulia Pagliaroli, and Francesco Lorenzo Villante. On the Goals of Neutrino Astronomy. *Nuovo Cim.*, 032C:353–359, 2009.

[4] Gian Luigi Fogli, E. Lisi, A. Marrone, and G. Scioscia. Super-Kamiokande data and atmospheric neutrino decay. *Phys. Rev.*, D59:117303, 1999.

[5] Carlo Giunti. Neutrino Flavor States and the Quantum Theory of Neutrino Oscillations. *AIP Conf. Proc.*, 1026:3–19, 2008.

[6] S. M. Bilenky. Neutrinoless Double Beta-Decay. *ArXiv e-prints*, January 2010.

[7] B. Kayser, F. Gibrat-Debu, and F. Perrier. The physics of massive neutrinos. *World Scientific Lecture Notes in Physics*, 25, 1989.

[8] H. Fritzsch and Z.-Z. Xing. Mass and Flavor Mixing Schemes of Quarks and Leptons. *Progress in Particle and Nuclear Physics*, 45:1–81, January 2000.

[9] C. Giunti. *Fundamentals of Neutrino Physics and Astrophysics*. Oxford university press, 2007.

[10] Stephen T. Thornton and Jerry B. Marion. *Classical dynamics of particles and systems*. Brooks/Cole, 2004.

[11] S. M. Bilenky, C. Giunti, J. A. Grifols, and E. Masso. Absolute Values of Neutrino Masses: Status and Prospects. *Phys. Rept.*, 379:69–148, 2003.

[12] Zhi-zhong Xing. Theoretical Overview of Neutrino Properties. *Int. J. Mod. Phys.*, A23:4255–4272, 2008.

[13] Yuval Grossman and Harry J. Lipkin. Flavor oscillations from a spatially localized source: A simple general treatment. *Phys. Rev.*, D55:2760–2767, 1997.

[14] Harry J. Lipkin. What is coherent in neutrino oscillations. *Phys. Lett.*, B579:355–360, 2004.

[15] Leo Stodolsky. The unnecessary wavepacket. *Phys. Rev.*, D58:036006, 1998.

[16] Yoshihiro Takeuchi, Yuichi Tazaki, S. Y. Tsai, and Takashi Yamazaki. How do neutrinos propagate? Wave packet treatment of neutrino oscillation. *Prog. Theor. Phys.*, 105:471–482, 2001.

[17] E. K. Akhmedov and A. Y. Smirnov. Paradoxes of neutrino oscillations. *Physics of Atomic Nuclei*, 72:1363–1381, August 2009.

[18] C. Giunti. Coherence and wave packets in neutrino oscillations. *Found. Phys. Lett.*, 17:103–124, 2004.

[19] Evgeny Kh. Akhmedov and Joachim Kopp. Neutrino oscillations: Quantum mechanics vs. quantum field theory. *JHEP*, 04:008, 2010.

[20] E. K. Akhmedov, J. Kopp, and M. Lindner. Oscillations of Mössbauer neutrinos. *Journal of High Energy Physics*, 5:5–+, May 2008.

[21] E. K. Akhmedov, J. Kopp, and M. Lindner. COMMENTS AND REPLIES: Comment on 'Time-energy uncertainty relations for neutrino oscillations and the Mössbauer neutrino experiment'. *Journal of Physics G Nuclear Physics*, 36(7):078001–+, July 2009.

[22] Boris Kayser and Joachim Kopp. Testing the wave packet approach to neutrino oscillations in future experiments. *ArXiv e-prints*, 2010.

[23] F. Boehm. Reactor Neutrino Physics – An Update. *ArXiv Nuclear Experiment e-prints*, June 1999.

[24] John G. Learned, Stephen T. Dye, and Sandip Pakvasa. Hanohano: A Deep ocean anti-neutrino detector for unique neutrino physics and geophysics studies. *ArXiv e-prints*, 2007.

[25] Boris Kayser. Neutrino mass, mixing, and flavor change. *ArXiv e-prints*, 2002.

[26] Particle Data Group. Leptons. `http://pdg.lbl.gov/2009/tables/rpp2009-sum-leptons.pdf`, 2009 (accessed June 7, 2010).

[27] Carlos Pena-Garay and Aldo Serenelli. Solar neutrinos and the solar composition problem. 2008.

[28] Rafael A. Garcia, Sylvaine Turck-Chieze, Sebastian J. Jimenez-Reyes, Jerome Ballot, Pere L. Palle, Antonio Eff-Darwich, Savita Mathur, and Janine Provost. Tracking Solar Gravity Modes: The Dynamics of the Solar Core. *Science*, 316(5831):1591–1593, 2007.

[29] M. Deniz et al. Measurement of Neutrino-Electron Scattering Cross-Section with a CsI(Tl) Scintillating Crystal Array at the Kuo-Sheng Nuclear Power Reactor. *Phys. Rev.*, D81:072001, 2010.